Hindawi
Journal of GeoEnergy
Volume 2023, Article ID 5745180, 14 pages
https://doi.org/10.1155/2023/5745180

Research Article

Effects of Reservoir Boundary Conditions, Drainage Shape, and Well Location on Productivity of a Vertical Well

Jing Lu,[1] **Erlong Yang**,[2] **Md. Motiur Rahman**,[2] **and Xueliang Wang**[1]

[1]*Key Lab of Enhanced Oil Recovery, Ministry of Education, Northeast Petroleum University, Daqing, China*
[2]*Department of Petroleum Engineering, Khalifa University of Science and Technology, Abu Dhabi, UAE*

Correspondence should be addressed to Jing Lu; 2590501988@qq.com

Received 17 February 2023; Revised 11 May 2023; Accepted 20 June 2023; Published 13 July 2023

Academic Editor: Youwei He

This paper gives a review of steady state and pseudosteady state productivity equations for an unfractured fully penetrating vertical well in a permeability anisotropic reservoir. This paper also studies the effects of drainage area, reservoir boundary conditions, drainage shape, and well location on productivity. The production performances of an unfractured vertical well in a circular reservoir, a sector fault reservoir and a rectangular reservoir are studied and compared. Mechanical skin factor is included in the productivity equations. This paper examines the steady state and pseudosteady state production performance of oil wells with constant flow rates in different drainage shapes, a library of productivity equations is introduced, several combinations of closed and/or constant pressure boundary conditions are considered at lateral reservoir boundaries. The equations introduced in this paper can be used to determine the economical feasibility of a drilling an unfractured fully penetrating vertical well. It is concluded that, drainage area and reservoir boundary conditions have significant effects on productivity of a well, and productivity is a weak function of drainage shape and well location.

1. Introduction

Well productivity is one of primary concerns in field development and provides the basis for field development strategy. To determine the economical feasibility of drilling a well, petroleum engineers need reliable methods to estimate its expected productivity. Petroleum engineers often relate the productivity evaluation to the long-time performance behavior of a well, that is, the behavior during pseudosteady state or steady state flow [1].

Substituting Darcy's equation into the equation of continuity, the steady state productivity equation for an unfractured fully penetrating vertical well in a permeability isotropic circular reservoir with constant pressure outer boundary is obtained below [2]:

$$Q_w = F_D \frac{2\pi kh(P_e - P_w)/(\mu B)}{\ln(R_e/R_w)}, \tag{1}$$

where k is reservoir permeability; h is payzone thickness; μ is oil viscosity; P_e, P_w are pressures at drainage outer boundary and wellbore, respectively; R_e, R_w are radii of drainage area and wellbore, respectively; Q_w is well flow rate; F_D is the unit conversion factor [3]. In oil field units, $F_D = 0.001127$ [4].

The pseudosteady state productivity equation for an unfractured fully penetrating vertical well in a permeability isotropic circular reservoir with closed outer boundary is given by [5]:

$$Q_w = F_D \frac{2\pi kh(P_a - P_w)/(\mu B)}{\ln(R_e/R_w) - 3/4}, \tag{2}$$

where P_a is the average reservoir pressure throughout the circular drainage area.

To account for irregular drainage shapes or asymmetrical positioning of a well within its drainage area, the following productivity equation was proposed by Dietz [6]:

$$Q_w = F_D \frac{2\pi kh(P_a - P_w)/(\mu B)}{(1/2)\ln[2.2458A/(C_A r_w^2)]}, \tag{3}$$

where C_A is shape factor and A is the drainage area.

Dietz [6] evaluated shape factor for rectangles with single well in various locations, but the shape factors obtained by Dietz are only applicable to rectangular shapes whose sides are integral ratios. Hagoort [7] presented an algorithm to calculate productivity of a well in a rectangle with arbitrary aspect ratio.

Well productivity is often evaluated using the productivity index, which is defined as the production rate per unit pressure drawdown [8]. Hagoort [9] presented an analytical formula for the stabilized productivity index of an arbitrary well in an arbitrary closed, naturally fractured reservoir that can be modeled as a double-porosity reservoir. Hagoort [10] also presented an algorithm to calculate the productivity index of a well with a vertical, infinite-conductivity fracture in a closed rectangular reservoir for a wide range of fracture lengths and reservoir aspect ratios. Friehauf et al. [11] developed a model to calculate the productivity index of a finite-conductivity fractured well, including the effect of fracture-face damage caused by fluid leakoff.

The production performance of multiple wells system has received attention in the last two decades.

Valko et al. [12] presented pseudosteady state productivity index for multiple wells producing from a closed rectangular reservoir. Umnuayponwiwat et al. [13] presented equations of inflow performance of multiple vertical and horizontal wells in closed systems. Marhaendrajana and Blasingame [14] presented a solution and associated analysis methodology to evaluate single well performance behavior in a multiple wells reservoir system.

Lu [1] presented steady state and pseudosteady state productivity equations for an off-center unfractured partially penetrating vertical well in a circular reservoir and a rectangular reservoir, but the mechanical skin factor due to formation damage or stimulation is not included in his equations.

The term *vertical well* in this paper is defined as a wellbore penetrating nearly vertically into a nearly horizontal, nonhydraulically fractured payzone [15].

A review of steady state and pseudosteady state productivity equations for an unfractured fully penetrating vertical well in a permeability anisotropic reservoir is given in this paper. The effects of drainage area, reservoir boundary conditions, drainage shape, and well location on productivity are also studied. The production performances of an unfractured vertical well in a circular reservoir, a sector fault reservoir, and a rectangular reservoir are compared. Several combinations of closed and/or constant pressure boundary conditions are considered at lateral reservoir boundaries, and mechanical skin factor is included in the productivity equations.

In this paper, all parameters of reservoir, wellbore, and fluid properties in the following equations are in oil field units as shown in Table 1. The unit conversion factor F_D in the following equations is equal to 0.001127, $F_D = 0.001127$.

Table 1: Oil field units for the parameters of reservoir, wellbore, and fluid properties.

Parameter	Oil field unit
Formation volume factor, B	bbl/STB
Pay zone thickness, h	ft
Permeability, k	mD
Pressure, P	psi
Productivity index, PI	STB/day/psi
Well flow rate, Q_w	STB/day
Off-center (off-vertex) distance, R_0	ft
Wellbore radius, R_w	ft
Drainage radius, R_e	ft
Length of rectangular reservoir, X_e	ft
Width of rectangular reservoir, Y_e	ft
Oil viscosity, μ	cp

2. Reservoir Boundary Conditions and Drainage Shape

In this paper, the following assumptions are made:

(1) The top and bottom boundaries of a three-dimensional reservoir are impermeable, and the reservoir is permeability anisotropic, the production occurs through an unfractured fully penetrating vertical well with radius R_w, thus the three-dimensional reservoir is reduced to a two-dimensional reservoir.

(2) Before production, the pressure is uniformly distributed in the reservoir, equal to the initial pressure P_i. If the reservoir has constant pressure boundaries (edge water, gas cap, and bottom water), the pressure P_e is equal to the initial value P_i at such boundaries during production.

(3) A single phase fluid, of small and constant compressibility C_f, constant viscosity μ, and formation volume factor B, flows from the reservoir to the well. Fluid properties are independent of pressure. Gravity forces are neglected.

(4) There is no water encroachment or water/gas coning. Edge water, gas cap, and bottom water are taken as constant pressure boundaries, multiphase flow effects are ignored.

In this paper, mechanical skin factor due to formation damage or stimulation is included in the productivity equations for an unfractured fully penetrating vertical well in a permeability anisotropic reservoir.

For an unfractured fully penetrating vertical well in an isotropic reservoir, if we refer to the additional pressure drop in the skin zone as ΔP_s, then [16]

$$\Delta P_s = \left(\frac{1}{F_D}\right)\left(\frac{\mu B Q_w}{2\pi k h}\right) S_m, \tag{4}$$

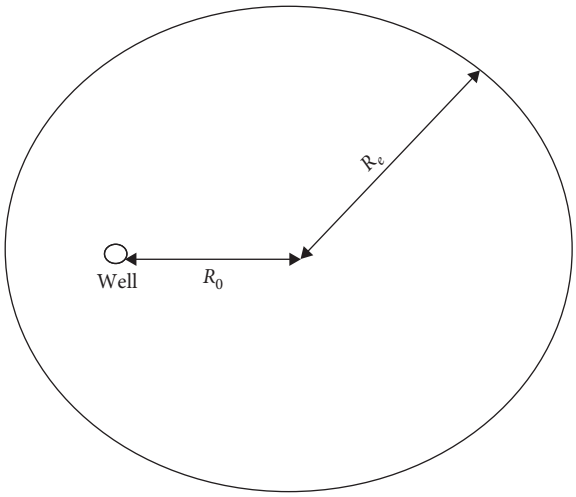

Figure 1: An off-center well in a circular reservoir.

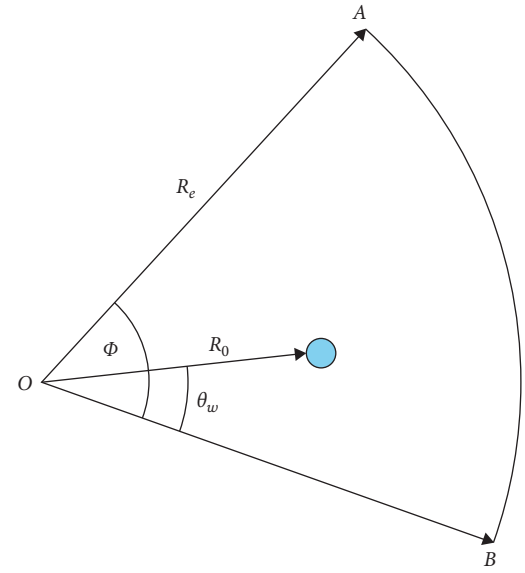

Figure 2: A well in a sector fault reservoir.

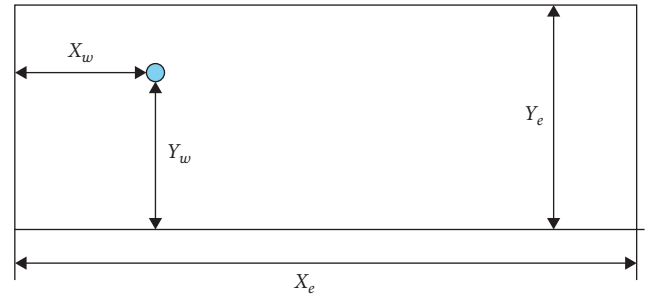

Figure 3: A well in a rectangular reservoir.

where S_m is mechanical skin factor due to formation damage or stimulation.

In a permeability anisotropic reservoir, there holds [3]

$$\Delta P_s = \left(\frac{1}{F_D}\right)\left(\frac{\mu B Q_w}{2\pi k_r h}\right) S_m, \tag{5}$$

k_r is the radial permeability. In a rectangular reservoir, we always assume $k_r = \sqrt{k_x k_y}$.

Figure 1 is a schematic of an off-center unfractured fully penetrating vertical well in a circular reservoir with radius R_e and the off-center distance is R_0. The following two cases of different lateral boundary conditions are considered for a circular reservoir:

Case 1: Constant pressure lateral boundary

$$P|_{r=R_e} = P_e = P_i. \tag{6}$$

Case 2: Impermeable lateral boundary

$$\left.\frac{\partial P}{\partial r}\right|_{r=R_e} = 0. \tag{7}$$

Figure 2 is a schematic of an unfractured fully penetrating vertical well in a sector fault reservoir with radius R_e, the well is on the bisector line, the well location angle $\theta_w = \Phi/2$, and sector angle $\Phi = \pi/n$, where n is an integer number, and R_0 is off-vertex distance of the well.

The two sides of the angle are impermeable, that is, the sector reservoir is with two sealing faults

$$\left.\frac{\partial P}{\partial N}\right|_{OA} = 0, \quad \left.\frac{\partial P}{\partial N}\right|_{OB} = 0, \tag{8}$$

where $\partial P/\partial N|_{OA,OB}$ are the exterior normal derivatives of pressure on the two sides of angle of the sector area.

Case 1: Constant pressure outer boundary

If the outer boundary is with edge water, during production the pressure at the outer boundary is always equal to initial reservoir pressure P_i.

$$P|_{r=R_e} = P_e = P_i. \tag{9}$$

Case 2: Outer boundary is impermeable

$$\left.\frac{\partial P}{\partial r}\right|_{r=R_e} = 0. \tag{10}$$

Figure 3 is a schematic of an off-center unfractured fully penetrating vertical well in a rectangular reservoir with length (x direction) X_e and width (y direction) Y_e. The original point of the rectangular coordinate system is the lower left corner point of the rectangular area, the well is located at the point (X_w, Y_w). And the following five cases of different lateral boundary conditions are applicable to a rectangular reservoir [17].

Case 1: the rectangular reservoir is surrounded by a strong edge water drive, such that the pressures at the four lateral boundaries are assumed constant and equal to the reservoir initial pressure during production

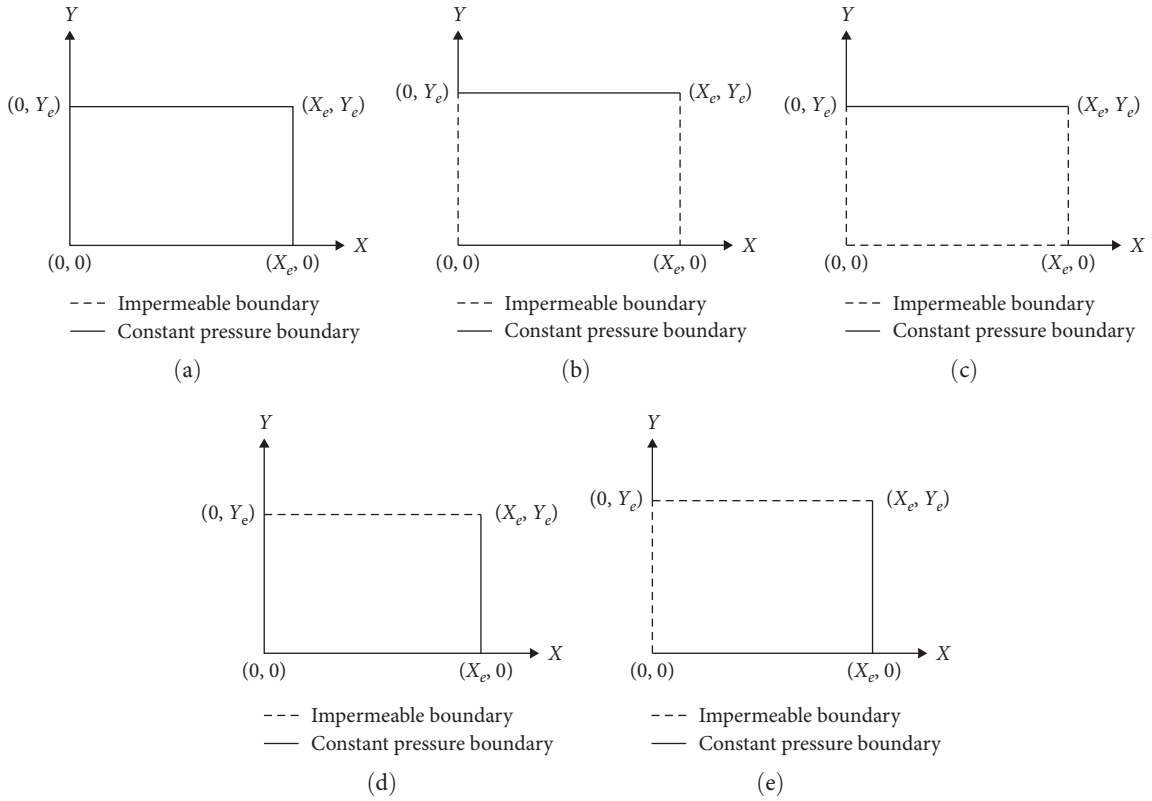

Figure 4: Lateral boundary conditions for rectangular reservoir: (a) Case 1, (b) Case 2, (c) Case 3, (d) Case 4, and (e) Case 5.

$$P|_{x=0} = P|_{x=X_e} = P|_{y=0} = P|_{y=Y_e} = P_e = P_i. \quad (11)$$

Case 2: Only two opposite lateral boundaries are at constant pressure. The other two opposite lateral boundaries are considered as no-flow (impermeable) boundaries

$$P|_{y=0} = P|_{y=Y_e} = P_e = P_i, \quad \left.\frac{\partial P}{\partial x}\right|_{x=0} = \left.\frac{\partial P}{\partial x}\right|_{x=X_e} = 0. \quad (12)$$

Case 3: Only one lateral boundary is at constant pressure, while the other three lateral boundaries are considered as no-flow (impermeable) boundaries

$$P|_{y=Y_e} = P_e = P_i, \quad \left.\frac{\partial P}{\partial x}\right|_{x=0} = \left.\frac{\partial P}{\partial x}\right|_{x=X_e} = \left.\frac{\partial P}{\partial y}\right|_{y=0} = 0. \quad (13)$$

Case 4: Only one lateral boundary is a no-flow (impermeable) boundary, while the other three are at constant pressure

$$P|_{x=0} = P|_{x=X_e} = P|_{y=0} = P_e = P_i, \quad \left.\frac{\partial P}{\partial y}\right|_{y=Y_e} = 0. \quad (14)$$

Case 5: Only two adjacent lateral boundaries are at constant pressure, while the other two adjacent lateral boundaries are no-flow (impermeable) boundaries

$$P|_{y=0} = P|_{x=X_e} = P_e = P_i, \quad \left.\frac{\partial P}{\partial x}\right|_{x=0} = \left.\frac{\partial P}{\partial y}\right|_{y=Y_e} = 0. \quad (15)$$

The above five different lateral boundary conditions in Case 1 through Case 5 are shown in Figure 4(a) through Figure 4(e), respectively.

3. Productivity Equations in Steady State

This section presents the steady state productivity equations for an unfractured fully penetrating vertical well located in a circular reservoir, a sector reservoir and a rectangular reservoir, and the mechanical skin factor is included.

3.1. Circular Reservoir. If an off-center unfractured fully penetrating vertical well is located in a permeability isotropic circular reservoir which has a constant pressure outer boundary, then the steady state productivity equation is [1]

$$Q_w = F_D \frac{2\pi kh(P_e - P_w)/(\mu B)}{\ln\left[(\mathrm{R}_e^2 - R_0^2)/(R_e R_w)\right] + S_m}, \quad (16)$$

where R_0 is off-center distance of the well, S_m is mechanical skin factor due to formation damage or stimulation, and F_D is the unit conversion factor. In oil field units, $F_D = 0.001127$.

If the well is in a permeability anisotropic reservoir, then

$$Q_w = F_D \frac{2\pi k_r h(P_e - P_w)/(\mu B)}{\ln\left[(R_{eD}^2 - R_{0D}^2)/(R_{eD}R_{wD})\right] + S_m}. \tag{17}$$

The definitions of R_{eD}, R_{oD}, R_{wD} are given in Appendix A.

For a well located at the center, the off-center distance $R_0 = 0$, then Equation (16) reduces to

$$Q_w = F_D \frac{2\pi kh(P_e - P_w)/(\mu B)}{\ln(R_e/R_w) + S_m}. \tag{18}$$

If $S_m = 0$, Equation (18) is equivalent to Equation (1), which is the well-known steady state productivity equation for an unfractured fully penetrating vertical well located at the center of a permeability isotropic circular reservoir in the literature [2].

3.2. Sector Fault Reservoir. If an unfractured fully penetrating vertical well is located in a permeability anisotropic sector fault reservoir with outer boundaries indicated in Equations (8) and (9), the well is on the bisector line, the well location angle $\theta_w = \Phi/2$, off-vertex distance is R_0, sector angle $\Phi = \pi/n$, and n is an integer number, we have

$$Q_w = F_D \frac{2\pi k_r h(P_i - P_w)/(\mu B)}{\ln(\Gamma) + S_m}, \tag{19}$$

where

$$\Gamma = \frac{(1 - R_{0D}^{2n})[1 - 2R_{0D}^{2n}\cos(2n\theta_w) + R_{0D}^{4n}]^{1/2}}{2nR_{wD}R_{0D}^{2n-1}\sin(n\theta_w)}, \tag{20}$$

Γ is sector shape function in steady state, the definitions of R_{oD}, R_{wD} are given in Appendix A.

If permeability is isotropic, $k_r = k$, consequently,

$$\Gamma = \frac{[1 - (R_0/R_e)^{2n}][1 - 2(R_0/R_e)^{2n}\cos(2n\theta_w) + (R_0/R_e)^{4n}]^{1/2}}{2n(R_w/R_0)(R_0/R_e)^{2n-1}\sin(n\theta_w)}, \tag{21}$$

then

$$Q_w = F_D \frac{2\pi kh(P_i - P_w)/(\mu B)}{\ln(\Gamma) + S_m}. \tag{22}$$

For $n = 1, 2, 3, 4, 5, 6, 8, 9, 10$, and Γ can be found in Table 2.

3.3. Rectangular Reservoir. If an off-center unfractured fully penetrating vertical well is located in a permeability isotropic rectangular reservoir which has at least one constant pressure outer boundary, we have the following five cases:

Table 2: Steady state sector shape functions for special sector angles.

Case	$\Phi = \pi/n$	n	θ_w	Γ
1	π	1	$\pi/2$	$[1 - (R_0/R_e)^4]/(2R_wR_0/R_e^2)$
2	$\pi/2$	2	$\pi/4$	$[1 - (R_0/R_e)^8]/(4R_wR_0^3/R_e^4)$
3	$\pi/3$	3	$\pi/6$	$[1 - (R_0/R_e)^{12}]/(6R_wR_0^5/R_e^6)$
4	$\pi/4$	4	$\pi/8$	$[1 - (R_0/R_e)^{16}]/(8R_wR_0^7/R_e^8)$
5	$\pi/5$	5	$\pi/10$	$[1 - (R_0/R_e)^{20}]/(10R_wR_0^9/R_e^{10})$
6	$\pi/6$	6	$\pi/12$	$[1 - (R_0/R_e)^{24}]/(12R_wR_0^{11}/R_e^{12})$
7	$\pi/8$	8	$\pi/16$	$[1 - (R_0/R_e)^{32}]/(16R_wR_0^{15}/R_e^{16})$
8	$\pi/9$	9	$\pi/18$	$[1 - (R_0/R_e)^{36}]/(18R_wR_0^{17}/R_e^{18})$
10	$\pi/10$	10	$\pi/20$	$[1 - (R_0/R_e)^{40}]/(20R_wR_0^{19}/R_e^{20})$

Case 1: The lateral boundary condition is defined by Equation (11), then [1]

$$Q_w = F_D \frac{2\pi kh(P_i - P_w)/(\mu B)}{1/2\ln[T_1 \times T_2/(T_3 \times T_4)] + S_m}, \tag{23}$$

where

$$T_1 = \sin^2(\pi Y_w/Y_e)/\sin^2[\pi R_w/(2Y_e)], \tag{24}$$

$$T_2 = [\sin^2(\pi Y_w/Y_e) + \sinh^2(\pi X_e/Y_e)]/\{\sin^2[\pi R_w/(2Y_e)] + \sinh^2(\pi X_e/Y_e)\}, \tag{25}$$

$$T_3 = [\sin^2(\pi Y_w/Y_e) + \sinh^2(\pi X_w/Y_e)]/\{\sin^2[\pi R_w/(2Y_e)] + \sinh^2(\pi X_w/Y_e)\}, \tag{26}$$

$$T_4 = \{\sin^2(\pi Y_w/Y_e) + \sinh^2[(\pi/Y_e)(X_e - X_w)]\}/\{\sin^2[\pi R_w/(2Y_e)] + \sinh^2[(\pi/Y_e)(X_e - X_w)]\}. \tag{27}$$

For a fully penetrating vertical well at the center of an isotropic square reservoir, we have $X_w = X_e/2 = Y_w = Y_e/2$, then Equation (23) can be approximated by the following expression

$$Q_w = F_D \frac{2\pi kh(P_i - P_w)/(\mu B)}{1/2\ln[\tau_1 \times \tau_2/(\tau_3 \times \tau_4)] + S_m}, \tag{28}$$

where

$$\tau_1 = 1.0/\sin^2[\pi R_w/(2Y_e)], \tag{29}$$

$$\tau_2 = [1 + \sinh^2(\pi)]/\{\sin^2[\pi R_w/(2Y_e)] + \sinh^2(\pi)\}, \tag{30}$$

$$\tau_3 = \tau_4 = [1 + \sinh^2(\pi/2)]/\{\sin^2[\pi R_w/(2Y_e)] + \sinh^2(\pi/2)\}. \tag{31}$$

Equation (28) is the steady state productivity equation for a fully penetrating vertical well located at the center of a permeability isotropic square reservoir surrounded by a strong aquifer.

Case 2: The lateral boundary condition is defined by Equation (12), then [17]

$$Q_w = F_D \frac{2\pi kh(P_i - P_w)/(\mu B)}{1/2\ln(T_1 \times T_2 \times T_3 \times T_4) + S_m}, \tag{32}$$

and T_1, T_2, T_3, and T_4 have the same meanings as in Equations (24)–(27), respectively.

Case 3: The lateral boundary condition is defined by Equation (13), then

$$Q_w = F_D \frac{2\pi kh(P_i - P_w)/(\mu B)}{1/2\ln(T_5 \times T_6 \times T_7 \times T_8) + S_m}, \tag{33}$$

where

$$\begin{aligned} T_5 = {} & [1 + 2\exp(-\pi X_w/Y_e)\cos(\pi Y_w/Y_e) + \exp(-2\pi X_w/Y_e)] \\ & \times\{1 + 2\exp(-\pi X_w/Y_e)\cos[\pi R_w/(2Y_e)] + \exp(-2\pi X_w/Y_e)\} \\ & \div[1 - 2\exp(-\pi X_w/Y_e)\cos(\pi Y_w/Y_e) + \exp(-2\pi X_w/Y_e)] \\ & \div\{1 - 2\exp(-\pi X_w/Y_e)\cos[\pi R_w/(2Y_e)] + \exp(-2\pi X_w/Y_e)\}, \end{aligned} \tag{34}$$

$$\begin{aligned} T_6 = {} & \{1 + 2\exp[-\pi(X_e - X_w)/Y_e]\cos(\pi Y_w/Y_e) + \exp[-2\pi(X_e - X_w)/Y_e]\} \\ & \times\{1 + 2\exp[-\pi(X_e - X_w)/Y_e]\cos[\pi R_w/(2Y_e)] + \exp[-2\pi(X_e - X_w)/Y_e]\} \\ & \div\{1 - 2\exp[-\pi(X_e - X_w)/Y_e]\cos(\pi Y_w/Y_e) + \exp[-2\pi(X_e - X_w)/Y_e]\} \\ & \div\{1 - 2\exp[-\pi(X_e - X_w)/Y_e]\cos[\pi R_w/(2Y_e)] + \exp[-2\pi(X_e - X_w)/Y_e]\}, \end{aligned} \tag{35}$$

$$T_7 = \frac{[1 + \cos(\pi Y_w/Y_e)]\{1 + \cos[\pi R_w/(2Y_e)]\}}{[1 - \cos(\pi Y_w/Y_e)]\{1 - \cos[\pi R_w/(2Y_e)]\}}, \tag{36}$$

$$\begin{aligned} T_8 = {} & [1 + 2\exp(-\pi X_e/Y_e)\cos(\pi Y_w/Y_e) + \exp(-2\pi X_e/Y_e)] \\ & \times\{1 + 2\exp(-\pi X_e/Y_e)\cos[\pi R_w/(2Y_e)] + \exp(-2\pi X_e/Y_e)\} \\ & \div[1 - 2\exp(-\pi X_e/Y_e)\cos(\pi Y_w/Y_e) + \exp(-2\pi X_e/Y_e)] \\ & \div\{1 - 2\exp(-\pi X_e/Y_e)\cos[\pi R_w/(2Y_e)] + \exp(-2\pi X_e/Y_e)\}. \end{aligned} \tag{37}$$

Case 4: The lateral boundary condition is defined by Equation (14), then

$$Q_w = F_D \frac{2\pi kh(P_i - P_w)/(\mu B)}{1/2\ln(T_9 \times T_{10} \times T_{11} \times T_{12}) + S_m}, \tag{38}$$

where

$$\begin{aligned} T_9 = {} & [1 + 2\exp(-\pi X_w/Y_e)\cos(\pi Y_w/Y_e) + \exp(-2\pi X_w/Y_e)] \\ & \times\{1 - 2\exp(-\pi X_w/Y_e)\cos[\pi R_w/(2Y_e)] + \exp(-2\pi X_w/Y_e)\} \\ & \div[1 - 2\exp(-\pi X_w/Y_e)\cos(\pi Y_w/Y_e) + \exp(-2\pi X_w/Y_e)] \\ & \div\{1 + 2\exp(-\pi X_w/Y_e)\cos[\pi R_w/(2Y_e)] + \exp(-2\pi X_w/Y_e)\}, \end{aligned} \tag{39}$$

$$\begin{aligned} T_{10} = {} & \{1 + 2\exp[-\pi(X_e - X_w)/Y_e]\cos(\pi Y_w/Y_e) + \exp[-2\pi(X_e - X_w)/Y_e]\} \\ & \times\{1 - 2\exp[-\pi(X_e - X_w)/Y_e]\cos[\pi R_w/(2Y_e)] + \exp[-2\pi(X_e - X_w)/Y_e]\} \\ & \div\{1 - 2\exp[-\pi(X_e - X_w)/Y_e]\cos(\pi Y_w/Y_e) + \exp[-2\pi(X_e - X_w)/Y_e]\} \\ & \div\{1 + 2\exp[-\pi(X_e - X_w)/Y_e]\cos[\pi R_w/(2Y_e)] + \exp[-2\pi(X_e - X_w)/Y_e]\}, \end{aligned} \tag{40}$$

$$T_{11} = \frac{[1 - \cos(\pi Y_w/Y_e)]\{1 + \cos[\pi R_w/(2Y_e)]\}}{[1 + \cos(\pi Y_w/Y_e)]\{1 - \cos[\pi R_w/(2Y_e)]\}}, \tag{41}$$

$$\begin{aligned} T_{12} = {} & [1 - 2\exp(-\pi X_e/Y_e)\cos(\pi Y_w/Y_e) + \exp(-2\pi X_e/Y_e)] \\ & \times\{1 + 2\exp(-\pi X_e/Y_e)\cos[\pi R_w/(2Y_e)] + \exp(-2\pi X_e/Y_e)\} \\ & \div[1 + 2\exp(-\pi X_e/Y_e)\cos(\pi Y_w/Y_e) + \exp(-2\pi X_e/Y_e)] \\ & \div\{1 - 2\exp(-\pi X_e/Y_e)\cos[\pi R_w/(2Y_e)] + \exp(-2\pi X_e/Y_e)\}. \end{aligned} \tag{42}$$

Case 5: The lateral boundary condition is defined by Equation (15), then

$$Q_w = F_D \frac{2\pi kh(P_i - P_w)/(\mu B)}{1/2\ln(T_{13} \times T_{14} \times T_{15} \times T_{16} \times T_{17} \times T_{18} \times T_{19} \times T_{20}) + S_m}, \tag{43}$$

where

$$\begin{aligned} T_{13} = {} & [1 - 2\exp(-\pi X_w/Y_e)\cos(\pi Y_w/Y_e) + \exp(-2\pi X_w/Y_e)] \\ & \times\{1 + 2\exp(-\pi X_w/Y_e)\cos[\pi R_w/(2Y_e)] + \exp(-2\pi X_w/Y_e)\} \\ & \div[1 + 2\exp(-\pi X_w/Y_e)\cos(\pi Y_w/Y_e) + \exp(-2\pi X_w/Y_e)] \\ & \div\{1 - 2\exp(-\pi X_w/Y_e)\cos[\pi R_w/(2Y_e)] + \exp(-2\pi X_w/Y_e)\}, \end{aligned} \tag{44}$$

$$\begin{aligned} T_{14} = {} & \{1 - 2\exp[-\pi(2X_e - X_w)/Y_{eD}]\cos(\pi Y_w/Y_e) + \exp[-2\pi(2X_e - X_w)/Y_e]\} \\ & \times\{1 + 2\exp[-\pi(2X_e - X_w)/Y_e]\cos[\pi R_w/(2Y_e)] + \exp[-2\pi(2X_e - X_w)/Y_e]\} \\ & \div\{1 + 2\exp[-\pi(2X_e - X_w)/Y_e]\cos(\pi Y_w/Y_e) + \exp[-2\pi(2X_e - X_w)/Y_e]\} \\ & \div\{1 - 2\exp[-\pi(2X_e - X_w)/Y_e]\cos[\pi R_w/(2Y_e)] + \exp[-2\pi(2X_e - X_w)/Y_e]\}, \end{aligned} \tag{45}$$

$$T_{15} = \frac{[1 - \cos(\pi Y_w/Y_e)]\{1 + \cos[\pi R_w/(2Y_e)]\}}{[1 + \cos(\pi Y_w/Y_e)]\{1 - \cos[\pi R_w/(2Y_e)]\}}, \tag{46}$$

$$\begin{aligned} T_{16} = {} & [1 - 2\exp(-2\pi X_e/Y_e)\cos(\pi Y_w/Y_e) + \exp(-4\pi X_e/Y_e)] \\ & \times\{1 + 2\exp(-2\pi X_e/Y_e)\cos[\pi R_w/(2Y_e)] + \exp(-4\pi X_e/Y_e)\} \\ & \div[1 + 2\exp(-2\pi X_e/Y_e)\cos(\pi Y_w/Y_e) + \exp(-4\pi X_e/Y_e)] \\ & \div\{1 - 2\exp(-2\pi X_e/Y_e)\cos[\pi R_w/(2Y_e)] + \exp(-4\pi X_e/Y_e)\}, \end{aligned} \tag{47}$$

$$\begin{aligned} T_{17} = {} & \{1 + 2\exp[-\pi(X_e - X_w)/Y_e]\cos(\pi Y_w/Y_e) + \exp[-2\pi(X_e - X_w)/Y_e]\} \\ & \times\{1 - 2\exp[-\pi(X_e - X_w)/Y_e]\cos[\pi R_w/(2Y_e)] + \exp[-2\pi(X_e - X_w)/Y_e]\} \\ & \div\{1 - 2\exp[-\pi(X_e - X_w)/Y_e]\cos(\pi Y_w/Y_e) + \exp[-2\pi(X_e - X_w)/Y_e]\} \\ & \div\{1 + 2\exp[-\pi(X_e - X_w)/Y_e]\cos[\pi R_w/(2Y_e)] + \exp[-2\pi(X_e - X_w)/Y_e]\}, \end{aligned} \tag{48}$$

$$\begin{aligned} T_{18} = {} & \{1 + 2\exp[-\pi(X_e + X_w)/Y_e]\cos(\pi Y_w/Y_e) + \exp[-2\pi(X_e + X_w)/Y_e]\} \\ & \times\{1 - 2\exp[-\pi(X_e + X_w)/Y_e]\cos[\pi R_w/(2Y_e)] + \exp[-2\pi(X_e + X_w)/Y_e]\} \\ & \div\{1 - 2\exp[-\pi(X_e + X_w)/Y_e]\cos(\pi Y_w/Y_e) + \exp[-2\pi(X_e + X_w)/Y_e]\} \\ & \div\{1 + 2\exp[-\pi(X_e + X_w)/Y_e]\cos[\pi R_w/(2Y_e)] + \exp[-2\pi(X_e + X_w)/Y_e]\}, \end{aligned} \tag{49}$$

$$\begin{aligned} T_{19} = {} & [1 + 2\exp(-\pi X_e/Y_e)\cos(\pi Y_w/Y_e) + \exp(-2\pi X_e/Y_e)] \\ & \times\{1 - 2\exp(-\pi X_e/Y_e)\cos[\pi R_w/(2Y_e)] + \exp(-2\pi X_e/Y_e)\} \\ & \div[1 - 2\exp(-\pi X_e/Y_e)\cos(\pi Y_w/Y_e) + \exp(-2\pi X_e/Y_e)] \\ & \div\{1 + 2\exp(-\pi X_e/Y_e)\cos[\pi R_w/(2Y_e)] + \exp(-2\pi X_e/Y_e)\}, \end{aligned} \tag{50}$$

$$\begin{aligned} T_{20} = {} & [1 + 2\exp(-\pi X_e/Y_e)\cos(\pi Y_w/Y_e) + \exp(-2\pi X_e/Y_e)] \\ & \times\{1 - 2\exp(-\pi X_e/Y_e)\cos[\pi R_w/(2Y_e)] + \exp(-2\pi X_e/Y_e)\} \\ & \div[1 - 2\exp(-\pi X_e/Y_e)\cos(\pi Y_w/Y_e) + \exp(-2\pi X_e/Y_e)] \\ & \div\{1 + 2\exp(-\pi X_e/Y_e)\cos[\pi R_w/(2Y_e)] + \exp(-2\pi X_e/Y_e)\}. \end{aligned} \tag{51}$$

Table 3: Pseudosteady state sector shape functions for special sector angles.

Case	$\Phi = 2\pi/m$	m	θ_w	Λ
1	π	2	$\pi/2$	$\ln\left[\frac{R_e^6}{2R_w R_0\left(R_e^2+R_0^2\right)\left(R_e^2-R_0^2-R_e^2R_0^2\right)}\right]+2\left(\frac{R_o}{R_e}\right)-3/2$
2	$2\pi/3$	3	$\pi/3$	$\ln\left[\frac{R_e^9}{3R_w R_0^2\left(R_e^2-R_0{}^2-R_eR_w\right)\left(R_e^4+R_e^2R_0^2+R_0^4\right)}\right]+3\left(\frac{R_o}{R_e}\right)-9/4$
3	$\pi/2$	4	$\pi/4$	$\ln\left[\frac{R_e^{12}}{4R_w R_0^3\left(R_e^2+R_0^2\right)\left(R_e^2-R_0^2-R_eR_w\right)\left(R_e^4+R_0^4\right)}\right]+4\left(\frac{R_o}{R_e}\right)-3$
4	$\pi/3$	6	$\pi/6$	$\ln\left[\frac{R_e^{10}}{6R_w R_0^5(R_e^2+R_0^2)(R_e^2-R_0^2-R_eR_w)}\right]$ $+\ln\left[\frac{R_e^8}{(R_e^4-R_e^2R_0^2+R_0^4)(R_e^4+R_e^2R_0^2+R_0^4)}\right]+6\left(\frac{R_o}{R_e}\right)-9/2$

If the reservoir is permeability anisotropic in the above five cases, then permeability k in Equations (23), (28), (32), (33), (38), and (43) should be replaced by $\sqrt{k_x k_y}$, and X_w, Y_w, X_e, Y_e, R_w in Equations (11), (29), (34), (35), (36), (37), (39), and (44) should be replaced by $X_{wD}, Y_{wD}, X_{eD}, Y_{eD}, R_{wD}$ which are given in Appendix A.

4. Productivity Equations in Pseudosteady State

If all reservoir boundaries are impermeable, and the producing time is sufficiently long, then the pseudosteady state can be reached [3], and the wellbore pressure must decline at the same rate as the average reservoir pressure. This section presents pseudosteady state productivity equations for an unfractured fully penetrating vertical well located in a permeability anisotropic circular reservoir, a sector fault reservoir, and a rectangular reservoir, and the mechanical skin factor is included.

4.1. Circular Reservoir. The productivity of an off-center unfractured fully penetrating vertical well in a permeability anisotropic closed circular reservoir in pseudosteady state can be calculated by [1]

$$Q_w = F_D \frac{2\pi k_r h(P_a - P_w)/(\mu B)}{\Psi + S_m}, \tag{52}$$

where

$$\Psi = \ln\left[\frac{R_{eD}^3}{R_{wD}(R_{eD}^2 - R_{0D}^2 - R_{0D}R_{wD})}\right] + \left(\frac{R_{oD}}{R_{eD}}\right)^2 - \frac{3}{4}, \tag{53}$$

and P_a is the average reservoir pressure throughout the circular drainage area, the definitions of R_{eD}, R_{oD}, R_{wD} are given in Appendix A.

If permeability is isotropic, $k_r = k$, consequently,

$$\Psi = \ln\left[\frac{R_e^3}{R_w(R_e^2 - R_0^2 - R_0R_w)}\right] + \left(\frac{R_o}{R_e}\right)^2 - \frac{3}{4}, \tag{54}$$

and

$$Q_w = F_D \frac{2\pi kh(P_a - P_w)/(\mu B)}{\Psi + S_m}. \tag{55}$$

For a well located at the center, the off-center distance $R_0 = 0$, then Equation (55) reduces to

$$Q_w = F_D \frac{2\pi kh(P_a - P_w)/(\mu B)}{\ln(R_e/R_w) - 3/4 + S_m}. \tag{56}$$

If $S_m = 0$, Equation (56) is equivalent to Equation (2), which is the well-known pseudosteady state productivity equation for an unfractured fully penetrating vertical well located at the center of a permeability isotropic closed circular reservoir in the literature [5].

4.2. Sector Fault Reservoir. If an unfractured fully penetrating vertical well is located in a permeability anisotropic closed sector fault reservoir with outer boundaries indicated in Equations (8) and (10), the well is on the bisector line, the well location angle $\theta_w = \Phi/2$ and sector angle $\Phi = 2\pi/m$, we have

$$Q_w = F_D \frac{2\pi k_r \mathrm{h}(P_a - P_w)/(\mu B)}{\ln(\Lambda) + S_m}, \tag{57}$$

where

$$\Lambda = m\left[\left(\frac{R_{oD}}{R_{eD}}\right)^2 - \frac{3}{4} + \ln\left(\frac{R_{eD}}{R_{oD}}\right)\right] + \ln\left[\frac{R_{oD}R_{eD}^2}{R_w(R_{eD}^2 - R_{oD}^2 - R_{oD}R_{wD})}\right] - \sum_{i=2}^{m} \ln\left\{\sqrt{\left\{1 - 2\left(\frac{R_{oD}}{R_{eD}}\right)^2 \cos\left[\frac{2(i-1)\pi}{m}\right] + \left(\frac{R_{oD}}{R_{eD}}\right)^4\right\}\left\{2 - 2\cos\left[\frac{2(i-1)\pi}{m}\right]\right\}}\right\}, \tag{58}$$

Λ is sector shape function in pseudosteady state, the definitions of R_{eD}, R_{oD}, R_{wD} are given in Appendix A.

$$\Lambda = m\left[\left(\frac{R_a}{R_e}\right)^2 - \frac{3}{4} + \ln\left(\frac{R_e}{R_0}\right)\right] + \ln\left[\frac{R_0 R_e^2}{R_w(R_e^2 - R_0^2 - R_0 R_w)}\right] - \sum_{i=2}^{m} \ln\left\{\sqrt{\left\{1 - 2\left(\frac{R_o}{R_e}\right)^2 \cos\left[\frac{2(i-1)\pi}{m}\right] + \left(\frac{R_o}{R_e}\right)^4\right\}\left\{2 - 2\cos\left[\frac{2(i-1)\pi}{m}\right]\right\}}\right\}, \tag{59}$$

and

$$Q_w = F_D \frac{2\pi kh(P_a - P_w)/(\mu B)}{\ln(\Lambda) + S_m}. \tag{60}$$

For $m = 2$, 3, 4, and 6, Λ can be found in Table 3.

4.3. Rectangular Reservoir. If an off-center unfractured fully penetrating vertical well is located inside a permeability anisotropic closed rectangular reservoir, then the well productivity in pseudosteady state can be calculated by [1]

$$Q_w = F_D \frac{2\pi\sqrt{k_x k_y}h(P_a - P_w)/(\mu B)}{\Theta + S_m}, \tag{61}$$

where P_a is average reservoir pressure throughout the rectangular drainage area, and

$$\Theta = \left(\frac{4\pi X_{eD}}{Y_{eD}}\right)\left(\frac{1}{6} - \frac{X_{wD}}{2X_{eD}} + \frac{X_{wD}^2}{2X_{eD}^2}\right) - \ln\left\{4\left|\sin\left(\pi Y_{wD}/Y_{eD}\right)\right|\sin\left[\pi R_{wD}/(2Y_{eD})\right]\right\}. \tag{62}$$

The definitions of $X_{wD}, Y_{wD}, X_{eD}, Y_{eD}, R_{wD}$ are given in Appendix A.

If permeability is isotropic, $k_x = k_y = k$, consequently,

$$Q_w = F_D \frac{2\pi kh(P_a - P_w)/(\mu B)}{\Theta + S_m}, \tag{63}$$

and

$$\Theta = \left(\frac{4\pi X_e}{Y_e}\right)\left(\frac{1}{6} - \frac{X_w}{2X_e} + \frac{X_w^2}{2X_e^2}\right) - \ln\left\{4\left|\sin\left(\pi Y_w/Y_e\right)\right|\sin\left[\pi R_w/(2Y_e)\right]\right\}. \tag{64}$$

If a well is located at the center of a closed rectangular reservoir,

$$X_w = X_e/2, \quad Y_w = Y_e/2, \tag{65}$$

If permeability is isotropic, $k_r = k$, consequently,

then Equation (63) reduces to

$$Q_w = F_D \frac{2\pi kh(P_a - P_w)/(\mu B)}{[\pi X_e/(6Y_e)] - \ln\{4\sin[\pi R_w/(2Y_e)]\} + S_m}. \tag{66}$$

If a well is at the center of a closed square reservoir, $X_e = Y_e$, then Equation (66) can be further simplified to

$$Q_w = F_D \frac{2\pi kh(P_a - P_w)/(\mu B)}{\pi/6 - \ln\{4\sin[\pi R_w/(2Y_e)]\} + S_m}. \tag{67}$$

Equation (67) is the pseudosteady state productivity equation for an unfractured fully penetrating vertical well located at the center of a permeability isotropic closed square reservoir.

Recall Equation (3), Dietz [6] developed the following equation to calculate the productivity of a vertical well in a permeability isotropic closed rectangular reservoir,

$$Q_w = F_D \frac{2\pi kh(P_a - P_w)/(\mu B)}{(1/2)\ln[2.2458(X_e Y_e)/(C_A r_w^2)]}, \tag{68}$$

where C_A is shape factor, which is used to account for asymmetrical positioning of a well within a rectangular reservoir.

5. Application and Analysis

All the above equations proposed by the authors of this paper are only applicable to an unfractured fully penetrating vertical well in a permeability anisotropic reservoir. The equations for partially penetrating vertical wells, horizontal wells, or hydraulically fractured wells will be available in our future work.

The performance of oil reservoirs is highly affected by many parameters, such as formation petrophysical properties, fluid properties, and reservoir and wellbore configuration. The effects of these parameters on reservoir performance are represented by productivity index (PI). PI is one of the major parameters in reservoir-management/development plans. It is defined as the surface production rate per unit pressure drawdown,

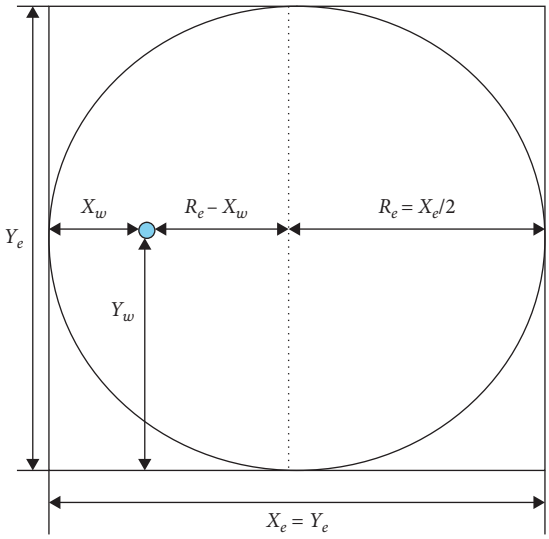

Figure 5: A square reservoir and its inscribed circle.

$$PI = \frac{Q_w}{\Delta P}. \tag{69}$$

In steady state, $\Delta P = P_i - P_w$ is constant with time; in pseudosteady state, $\Delta P = P_a - P_w$ is also constant with time. Thus, in steady state and pseudosteady state, unless the conditions progressively deteriorate because of formation damage and skin factor, PI is constant.

5.1. Effects of Drainage Shape and Well Location

Example 1. Figure 5 shows a square reservoir $(X_e = Y_e)$ and its inscribed circular reservoir. A fully penetrating vertical well is located at (X_w, Y_w) in the square reservoir. Assume $Y_w = Y_e/2 = X_e/2$ and X_w is variable. Calculate steady state productivity indexes if the square reservoir is with constant pressure outer boundary. And calculate the productivity indexes of the well which is located in the inscribed circular reservoir with constant pressure outer boundary. Reservoir and fluid properties data in field units are given in Table 4. Mechanical skin factor $S_m = 0$.

5.1.1. Solution. We use Equations (8) and (23), and note that

$$R_e = Y_e/2 = X_e/2 = Y_w,\ R_0 = X_e/2 - X_w = R_e - X_w. \tag{70}$$

Steady state productivity indexes of the well are given in Table 5.

Example 2. If the outer boundaries are impermeable in Figure 5, calculate the productivity indexes in pseudosteady state. Reservoir and fluid properties data are the same as those given in Table 4.

Table 4: Reservoir and fluid properties data for Examples 1 and 2.

Reservoir length, X_e	2,000 ft
Reservoir width, Y_e	2,000 ft
Wellbore radius, R_w	0.5 ft
Well location in y direction, Y_w	1,000 ft
Payzone thickness, h	50 ft
Permeability, k	200 mD
Oil Viscosity, μ	2.0 cp
Formation volume factor, B	1.1 RB/STB
Mechanical skin factor, S_m	0

Table 5: Steady state productivity indexes for Example 1.

Square reservoir		Inscribed circular reservoir	
X_w (ft)	PI (STB/day/psi)	$R_0 = R_e - X_w$ (ft)	PI (STB/day/psi)
100	5.38	900	5.42
200	4.84	800	4.89
300	4.59	700	4.65
400	4.44	600	4.50
500	4.35	500	4.40
600	4.28	400	4.33
700	4.24	300	4.29
800	4.21	200	4.26
900	4.20	100	4.24
1,000	4.20	0	4.24

Table 6: Pseudosteady state productivity indexes for Example 2.

Square reservoir		Inscribed circular reservoir	
X_w (ft)	PI (STB/day/psi)	$R_0 = R_e - X_w$ (ft)	PI (STB/day/psi)
100	3.90	900	3.45
200	4.03	800	3.78
300	4.15	700	4.02
400	4.27	600	4.20
500	4.37	500	4.36
600	4.45	400	4.48
700	4.52	300	4.58
800	4.57	200	4.64
900	4.60	100	4.69
1,000	4.61	0	4.70

5.1.2. Solution. We use Equations (21) and (63), pseudosteady state productivity indexes are given in Table 6.

Tables 5 and 6 indicate that in steady state and in pseudosteady state, the productivity index is a weak function of drainage shape and well location, neither drainage shape nor well location has significant effects on the production performance of a well.

Steady state is dominated by a constant pressure outer boundary flow regime, which implies that the same volume of fluid is being moved at the wellbore and at the outer boundary. Table 5 indicates that in steady state, for a given well, when the off-center distance increases (when R_0 increases and X_w decreases) the productivity index also increases. Because

Table 7: Steady state and pseudosteady state productivity indexes for Example 3.

Steady State		Pseudo-steady state	
Φ	PI (STB/day/psi)	Φ	PI (STB/day/psi)
π	4.27	π	4.83
$\pi/2$	3.88	$\pi/2$	5.11
$\pi/3$	3.47	$\pi/3$	5.13

Table 8: Steady state productivity indexes for Example 4.

	PI (STB/day/psi)
Case 1	4.20
Case 2	4.01
Case 3	3.40
Case 4	4.05
Case 5	3.85

the off-center well is near the constant pressure outer boundary, under the same pressure drop, the fluid moves through a short distance into the off-center well, consequently the productivity index is higher [8].

Pseudosteady state is dominated by a closed outer boundary flow regime, the produced fluid is evenly distributed in the reservoir. There is a zero flow rate at the closed outer boundary and maximum flow rate at the wellbore. Table 6 indicates that in pseudosteady state, for a given well, when the off-center distance increases, (when R_0 increases and Xw decreases), the productivity index decreases. Because in pseudosteady state, no driving force is from the closed outer boundary, for a well located at the center of a closed reservoir, all flowlines toward the wellbore are radial or parallel to each other, no curved flowlines; but for an off-center well, the flowlines toward the wellbore are curved, more energy is dissipated under the same pressure drop, and consequently the productivity index is smaller [18].

5.2. Effects of Drainage Area

Example 3. A fully penetrating vertical well is located on the bisector line of a sector fault reservoir.

The sector radius $R_e = 1000\,ft$, the off-vertex distance $R_0 = 500\,ft$, wellbore radius $R_w = 0.5\,ft$, other reservoir, and fluid properties data are the same as those given in Table 4. Mechanical skin factor $S_m = 0$. Calculate the steady state and pseudosteady state productivity index when the sector angle $\Phi = \pi, \pi/2, \pi/3$.

5.2.1. Solution. The equations in Table 2 and 3 are used in Equations (22) and (60), the productivity indexes are given in Table 7. Table 7 indicates that in steady state and in pseudosteady state, the productivity index is a strong function of drainage area.

As shown in Table 7, when the sector angle Φ decreases, steady state productivity index decreases. Because when Φ decreases, the drainage area also decreases, the length of the constant pressure outer boundary decreases, the driving force from the outer boundary decreases, and consequently the productivity index decreases.

Table 7 also indicates that in pseudosteady state, when the sector angle Φ decreases, the productivity index increases. No driving force is on the closed outer boundary, the produced fluid is evenly distributed in the reservoir. When Φ decreases, the drainage area also decreases, the fluid moves through a shorter distance into the wellbore, less energy is dissipated under the same pressure drop, and consequently the productivity index increases.

5.3. Effects of Reservoir Boundary Conditions

Example 4. A fully penetrating vertical well is located at the center of a square reservoir. Reservoir and fluid properties data are the same as those given in Table 4. Mechanical skin factor $S_m = 0$. Calculate the steady state productivity index for each case in Figure 4.

5.3.1. Solution. The well is located at the center of the square reservoir, we have $X_w = Y_w = Y_e/2 = X_e/2 = 1000\,ft$, for the five cases in Figure 4, by using Equations (23), (32), (33), (38), and (43), we can obtain the productivity indexes shown in Table 8.

Table 8 indicates that reservoir boundary conditions have significant effects on the production performance of a well.

As shown in Table 8, the productivity index of Case 1 is the biggest in the five cases as shown in Figure 4, and the productivity index of Case 3 is the smallest. Because all outer boundaries are at constant pressure for Case 1, the driving forces are from four boundaries, consequently the productivity index is the biggest. For Case 3, only one constant pressure outer boundary, the driving force is only from one outer boundary, thus the productivity index is the smallest in the five cases. Three constant pressure outer boundaries for Case 4, thus the productivity index is the second biggest. For Case 2 and Case 5, only two outer boundaries are at constant pressure, thus their productivity indexes are with intermediate values.

5.4. The Comparisons of Lu's Method and Dietz's Method

Example 5. A fully penetrating vertical well is located at the center of a closed rectangular reservoir. Reservoir width $Y_e = 2000\ ft$, other reservoir data and fluid properties data are the same as those given in Table 4. Mechanical skin factor $S_m = 0$. If aspect ratio $X_e/Y_e = 1, 2, 4, 5, 4.5$, calculate the pseudosteady state productivity index by Lu's method and Dietz's method.

5.4.1. Solution. When $X_e/Y_e = 1$, we use Equation (67) to calculate the productivity index, then

Table 9: Comparisons of productivity index of a well at the center of a closed rectangular reservoir calculated by Dietz's method and Lu's method.

Aspect ratio	Shape factor	PI calculated by Dietz's Method (Equation 68) (STB/day/psi)	PI calculated by Lu's Method (Equation 66) (STB/day/psi)
1	30.9	4.609	4.612
2	22.6	4.299	4.289
4	5.38	3.764	3.764
5	2.36	3.547	3.547
4.5	N/A	N/A	3.653

$$\begin{aligned} \mathrm{PI} &= \frac{0.001127 \times [2\pi kh/(\mu B)]}{\pi/6 - \ln\{4\sin[\pi R_w/(2Y_e)]\}} \\ &= \frac{0.001127 \times [2\pi \times 200 \times 50/(2.0 \times 1.1)]}{\pi/6 - \ln\{4\sin[\pi \times 0.5/(2 \times 2000)]\}} \\ &= 4.612\ (\mathrm{STB/day/psi}). \end{aligned} \tag{71}$$

For a well located at the center of a closed square reservoir, shape factor C_A is equal to 30.9 (Dietz, 1965), Equation (68) is used to calculate the productivity index,

$$\begin{aligned} \mathrm{PI} &= \frac{0.001127 \times [2\pi kh/(\mu B)]}{(1/2)\ln[2.2458(X_eY_e)/(C_Ar_w^2)]} \\ &= \frac{0.001127 \times [2\pi \times 200 \times 50/(2 \times 1.1)]}{0.5 \times \ln[2.2458 \times 2000^2/(30.9 \times 0.5^2)]} \\ &= 4.609\ (\mathrm{STB/day/psi}). \end{aligned} \tag{72}$$

When $X_e/Y_e = 2$, we use Equation (66),

$$\begin{aligned} \mathrm{PI} &= \frac{0.001127 \times [2\pi kh/(\mu B)]}{\pi X_e/(6Y_e) - \ln\{4\sin[\pi R_w/(2Y_e)]\}} \\ &= \frac{0.001127 \times [2\pi \times 200 \times 50/(2.0 \times 1.1)]}{2\pi/6 - \ln\{4\sin[\pi \times 0.5/(2 \times 2000)]\}} \\ &= 4.289\ (\mathrm{STB/day/psi}). \end{aligned} \tag{73}$$

When $X_e/Y_e = 2$, shape factor C_A is equal to 22.6 [6], then

$$\begin{aligned} \mathrm{PI} &= \frac{0.001127 \times [2\pi kh/(\mu B)]}{(1/2)\ln[2.2458(X_eY_e)/(C_Ar_w^2)]} \\ &= \frac{0.001127 \times [2\pi \times 200 \times 50/(2 \times 1.1)]}{0.5 \times \ln[2.2458 \times 4000 \times 2000/(20.6 \times 0.5^2)]} \\ &= 4.299\ (\mathrm{STB/day/psi}). \end{aligned} \tag{74}$$

When aspect ratio $X_e/Y_e = 4, 5$, the calculation results are shown in Table 9, we can find that little difference between the results in each case obtained by the two methods.

If $X_e/Y_e = 4.5$, we have

$$\begin{aligned} \mathrm{PI} &= \frac{0.001127 \times [2\pi kh/(\mu B)]}{\pi X_e/(6Y_e) - \ln\{4\sin[\pi R_w/(2Y_e)]\}} \\ &= \frac{0.001127 \times [2\pi \times 200 \times 50/(2.0 \times 1.1)]}{4.5\pi/6 - \ln\{4\sin[\pi \times 0.5/(2 \times 2000)]\}} \\ &= 3.653\ (\mathrm{STB/day/psi}). \end{aligned} \tag{75}$$

Dietz's method can not be used to calculate PI when $X_e/Y_e = 4.5$.

It must be pointed out the shape factors obtained by Dietz are only applicable to rectangular shapes whose sides are integral ratios, that is $X_e/Y_e = 1, 2, 4, 5$, but our proposed equations are applicable to a rectangular reservoir with arbitrary aspect ratio, shape factors are not required.

6. Summary

The disadvantage of steady state and pseudosteady state productivity equations in the literature is that those equations are only applicable to permeability isotropic reservoirs. The advantage of the productivity equations given by the authors of this paper is that the proposed equations are applicable to permeability anisotropic reservoir and can be used to study the effects of drainage area, reservoir boundary conditions, drainage shape, and well location on steady state and pseudosteady state productivity.

Another advantage of the productivity equations given by the authors is that the proposed equations are applicable to a well arbitrarily located in a circular reservoir and a rectangular reservoir. A summary of productivity equations for a permeability isotropic reservoir is given in Table 10.

The disadvantage of the productivity equation and the shape factors obtained by Dietz [6] is that Dietz's equation and shape factors are only applicable to rectangular shapes whose sides are integral ratios. The advantage of the equations given by the authors of this paper is that the proposed equations are applicable to a rectangular reservoir with arbitrary aspect ratio. The equations proposed by the authors can calculate the productivity of a well directly, shape factors are not required, thus shape factors for a rectangular reservoir is out of date.

Table 10: Summary of productivity equations for permeability isotropic reservoirs.

Circular reservoir		Rectangular reservoir	
Steady state, off-center well	Equation (16)	Steady state, four boundaries at constant pressure	Equations (23), (24)–(27)
Steady state, centered well	Equation (18)	Steady state, two opposite boundaries at constant pressure	Equations (32), (24)–(27)
Pseudosteady state, off-center well	Equations (54) and (55)	Steady state, only one boundary at constant pressure	Equations (33), (34)–(37)
Pseudo-steady state, centered well	Equation (56)	Steady state, three boundaries at constant pressure	Equations (38), (39)–(42)
Sector fault reservoir		Steady state, two adjacent boundaries at constant pressure	Equations (43), (44)–(51)
Steady state, well on bisector line	Equations (21) and (22)	Pseudosteady state, off-center well	Equations (63) and Eq. (64)
Pseudosteady state, well on bisector line	Equations (59) and (60)	Pseudosteady state, centered well	Equation (66)

7. Conclusions

(1) Drainage area and reservoir boundary conditions have significant effects on productivity, and the productivity index is a weak function of drainage shape and well location.

(2) In steady state, for a well in a circular reservoir or a rectangular reservoir, when off-center distance increases, the productivity index also increases.

(3) In pseudosteady state, for a well in a circular reservoir or a rectangular reservoir, when off-center distance increases, the productivity index decreases.

(4) In steady state, for a well in a sector fault reservoir, when sector angle decreases, the productivity index decreases.

(5) In pseudosteady state, for a well in a sector fault reservoir, when sector angle decreases, the productivity index increases.

(6) In steady state, for a given well in a square reservoir, when the number of constant pressure outer boundaries increases, the productivity index will also increase.

Nomenclature

B: Formation volume factor, bbl/STB
$\cos(.)$: Cosine function
$\cosh(.)$: Hyperbolic cosine function
$\exp(.)$: Exponential function
F_D: Unit conversion factor, dimensionless
h: Pay zone thickness, ft
k: Permeability, mD
P: Pressure, psi
PI: Productivity index, $STB/\text{day}/psi$
Q_w: Well flow rate, STB/day
R_0: Off-center (off-vertex) distance, ft
R_w: Wellbore radius, ft
R_e: Drainage radius, ft
S_m: Mechanical skin factor, fraction
$\sin(.)$: Sine function
$\sinh(.)$: Hyperbolic sine function
X_e: Length of rectangular reservoir, ft
X_w: Well location in X direction in rectangular reservoir, ft
Y_e: Width of rectangular reservoir, ft
Y_w: Well location in Y direction in rectangular reservoir, ft.

Greek Symbols

φ: Porosity, fraction
μ: Fluid viscosity, cp
θ_w: Well location angle, radians
τ_1: A function defined by Equation (29)
τ_2: A function defined by Equation (30)
τ_3: A function defined by Equation (31)
τ_4: A function defined by Equation (31)
Ω: Drainage domain
Γ: Steady state sector shape function defined by Equations (20) and (21)
Ψ: A function defined by Equations (53) and (54)
Θ: A function defined by Equations (62) and (64)
Φ: Sector angle, radians
Λ: pseudosteady state sector shape function defined by Equations (58) and (59).

Subscripts

a: Average
D: Dimensionless
e: External
i: Initial
r: Radial
w: Well.

Appendix

A. Definition of Dimensionless Parameters

For a circular reservoir and a sector fault reservoir, define average permeability as below:

$$k_a = k_r^{2/3} k_v^{1/3}, \tag{A.1}$$

where k_r is radial permeability and k_v is vertical permeability.

And define

$$R_{eD} = \left(\frac{k_a}{k_r}\right)^{1/2},\ R_{0D} = \left(\frac{R_0}{R_e}\right)\left(\frac{k_a}{k_r}\right)^{1/2},\ R_{wD} = \left(\frac{R_w}{R_e}\right)\left(\frac{k_a}{k_r}\right)^{1/2}. \tag{A.2}$$

For a rectangular reservoir, define average permeability and radial permeability as below:

$$k_a = \left(k_x k_y k_z\right)^{1/3}, \tag{A.3}$$

$$k_r = \left(k_x k_y\right)^{1/2}. \tag{A.4}$$

And define

$$X_{wD} = \left(\frac{X_w}{h}\right)\left(\frac{k_a}{k_x}\right)^{1/2},\ Y_{wD} = \left(\frac{Y_w}{h}\right)\left(\frac{k_a}{k_y}\right)^{1/2}, \tag{A.5}$$

$$X_{eD} = \left(\frac{X_e}{h}\right)\left(\frac{k_a}{k_x}\right)^{1/2},\ Y_{eD} = \left(\frac{Y_e}{h}\right)\left(\frac{k_a}{k_y}\right)^{1/2}, \tag{A.6}$$

$$R_{wD} = \left(\frac{R_w}{h}\right)\left(\frac{k_a}{\sqrt{k_x k_y}}\right)^{1/2}. \tag{A.7}$$

Data Availability

All data are contained within the article.

Conflicts of Interest

The authors declare that they have no conflicts of interest.

Authors' Contributions

Jing Lu established the model, derived the equations, and wrote the manuscript. Erlong Yang obtained financial support from the Hainan province Science and Technology Special Fund and Heilongjiang Postdoctoral Scientific Research Fund, he also supervised this research project. Md Motiur Rahman improved and revised the manuscript. Xueliang Wang analyzed data and drew the figures.

Acknowledgments

Authors acknowledge the financial support provided by the Hainan province Science and Technology Special Fund (ZDYF2022SHFZ107) and Heilongjiang Postdoctoral Scientific Research Fund (LBH-Q21012).

References

[1] J. Lu, *Productivity Equations for Oil Wells in Anisotropic Reservoirs*, PhD Dissertation, The University of Oklahoma, 2008.

[2] D. Tiab and E. C. Donaldson, *Petrophysics*, Elsevier—Gulf Professional Publishing, Burlington, Massachusetts, USA, 2004.

[3] J. Lee, J. B. Rollins, and J. P. Spivey, *Pressure Transient Testing*, Society of Petroleum Engineers, Richardson, Texas, USA, 2003.

[4] R. M. Butler, *Horizontal Wells for the Recovery of Oil, Gas and Bitumen*, Canadian Institute of Mining, Metallurgy and Petroleum, Calgary, Canada, 1994.

[5] B. C. Craft and M. Hawkins, *Applied Petroleum Reservoir Engineering*, Prentice Hall, Upper Saddle River, New Jersey, USA, 1991.

[6] D. N. Dietz, "Determination of average reservoir pressure from build-up surveys," *Journal of Petroleum Technology*, vol. 17, no. 8, pp. 955–959, 1965.

[7] J. Hagoort, "Semisteady-state productivity of a well in a rectangular reservoir producing at constant rate or constant pressure," *SPE Reservoir Evaluation & Engineering*, vol. 14, no. 6, pp. 677–686, 2011.

[8] T. Ahmed, *Reservoir Engineering Handbook*, Elsevier—Gulf Professional Publishing, Burlington, Massachusetts, USA, 2010.

[9] J. Hagoort, "Stabilized well productivity in double-porosity reservoirs," *SPE Reservoir Evaluation & Engineering*, vol. 11, no. 5, pp. 940–947, 2008.

[10] J. Hagoort, "The productivity of a well with a vertical infinite-conductivity fracture in a rectangular closed reservoir," *SPE Journal*, vol. 14, no. 4, pp. 715–720, 2009.

[11] K. E. Friehauf, A. Suri, and M. M. Sharma, "A simple and accurate model for well productivity for hydraulically fractured wells," *SPE Production & Operations*, vol. 25, no. 4, pp. 453–460, 2010.

[12] P. P. Valkó, L. E. Doublet, and T. A. Blasingame, "Development and application of the multiwell productivity index (MPI)," *SPE Journal*, vol. 5, no. 1, pp. 21–31, 2000.

[13] S. Umnuayponwiwat, E. Ozkan, and R. Raghavan, "Pressure transient behavior and inflow performance of multiple wells in closed systems," in *SPE Annual Technical Conference and Exhibition*, OnePetro, Dallas, Texas, October, 2000.

[14] T. Marhaendrajana and T. A. Blasingame, "Decline curve analysis using type curves—evaluation of well performance behavior in a multiwell reservoir system," in *SPE Annual Technical Conference and Exhibition*, OnePetro, New Orleans, Louisiana, 2001.

[15] B. Guo, *Well Productivity Handbook*, Gulf Professional Publishing, Houston, Texas, USA, 2019.

[16] M. J. Economides, A. D. Hill, and C. A. Ehligh-Economides, *Petroleum Production Systems*, Prentice Hall, Upper Saddle River, New Jersey, USA, 1994.

[17] J. Owayed, J. Lu, and D. Tiab, "Multiple-wells system productivity equations in a rectangular reservoir," *Journal of Engineering Research*, vol. 1, no. 1, pp. 235–260, 2013.

[18] T. Ahmed and P. D. McKinney, *Advanced Reservoir Engineering*, Elsevier—Gulf Professional Publishing, Burlington, Massachusetts, USA, 2005.